Controls on dissolved cobalt in surface waters of the Sargasso Sea: Comparisons with iron and aluminum

R. U. Shelley,[1,2,3] P. N. Sedwick,[4] T. S. Bibby,[5] P. Cabedo-Sanz,[2] T. M. Church,[6] R. J. Johnson,[7] A. I. Macey,[5] C. M. Marsay,[5] E. R. Sholkovitz,[8] S. J. Ussher,[2,7] P. J. Worsfold,[2] and M. C. Lohan[1,2]

Received 4 July 2011; revised 29 February 2012; accepted 6 April 2012; published 19 May 2012.

[1] Dissolved cobalt (dCo), iron (dFe) and aluminum (dAl) were determined in water column samples along a meridional transect (~31°N to 24°N) south of Bermuda in June 2008. A general north-to-south increase in surface concentrations of dFe (0.3–1.6 nM) and dAl (14–42 nM) was observed, suggesting that aerosol deposition is a significant source of dFe and dAl, whereas no clear trend was observed for near-surface dCo concentrations. Shipboard aerosol samples indicate fractional solubility values of 8–100% for aerosol Co, which are significantly higher than corresponding estimates of the solubility of aerosol Fe (0.44–45%). Hydrographic observations and analysis of time series rain samples from Bermuda indicate that wet deposition accounts for most (>80%) of the total aeolian flux of Co, and hence a significant proportion of the atmospheric input of dCo to our study region. Our aerosol data imply that the atmospheric input of dCo to the Sargasso Sea is modest, although this flux may be more significant in late summer. The water column dCo profiles reveal a vertical distribution that predominantly reflects 'nutrient-type' behavior, versus scavenged-type behavior for dAl, and a hybrid of nutrient- and scavenged-type behavior for dFe. Mesoscale eddies also appear to impact on the vertical distribution of dCo. The effects of biological removal of dCo from the upper water column were apparent as pronounced sub-surface minima (21 ± 4 pM dCo), coincident with maxima in *Prochlorococcus* abundance. These observations imply that *Prochlorococcus* plays a major role in removing dCo from the euphotic zone, and that the availability of dCo may regulate *Prochlorococcus* growth in the Sargasso Sea.

Citation: Shelley, R. U., et al. (2012), Controls on dissolved cobalt in surface waters of the Sargasso Sea: Comparisons with iron and aluminum, *Global Biogeochem. Cycles*, *26*, GB2020, doi:10.1029/2011GB004155.

1. Introduction

[2] Cobalt (Co) is an important micronutrient for marine phytoplankton [*Morel et al.*, 1994; *Croft et al.*, 2005]. While it is widely accepted that iron (Fe) supply can limit phytoplankton growth over large areas of the surface ocean [e.g., *Coale et al.*, 1996; *Boyd et al.*, 2000], there is increasing evidence to suggest that the availability of other trace elements such as Co may limit or co-limit algal growth in some oceanic regions [*Saito et al.*, 2008]. Indeed, a number of recent studies have recognized the importance and influence of Co on phytoplankton dynamics in the open ocean [e.g., *Saito et al.*, 2002, 2004, 2005; *Bertrand et al.*, 2007; *Panzeca et al.*, 2008; *Saito and Goepfert*, 2008].

[3] Cobalt is required for the synthesis of vitamin B_{12} by marine prokaryotes. Vitamin B_{12} is a cobalt-containing organometallic compound that is only produced by certain bacteria and archaea, hence eukaryotes must either acquire it from the environment, or follow metabolic pathways that do not require vitamin B_{12} [*Bertrand et al.*, 2007]. Cobalt is also a co-factor in the enzyme carbonic anhydrase (CA), which is required by marine phytoplankton for inorganic carbon acquisition [*Lane and Morel*, 2000]. Some eukaryotic phytoplankton are able to substitute Co or cadmium for zinc in CA, however some marine phytoplankton, such as the cyanobacteria *Prochlorococcus* and *Synechococcus*, have an

[1]Marine Institute, University of Plymouth, Plymouth, UK.
[2]School of Geography, Earth and Environmental Sciences, University of Plymouth, Plymouth, UK.
[3]Now at School of Earth, Ocean and Atmospheric Science, Florida State University, Tallahassee, Florida, USA.
[4]Ocean, Earth and Atmospheric Sciences, Old Dominion University, Norfolk, Virginia, USA.
[5]School of Ocean and Earth Science, University of Southampton, National Oceanography Centre, Southampton, UK.
[6]College of Marine and Earth Studies, University of Delaware, Newark, Delaware, USA.
[7]Bermuda Institute of Ocean Sciences, St. George's, Bermuda.
[8]Department of Marine Chemistry and Geochemistry, Woods Hole Oceanographic Institution, Woods Hole, Massachusetts, USA.

Corresponding author: R. U. Shelley, School of Earth, Ocean and Atmospheric Science, Florida State University, Tallahassee, FL 32306, USA. (rshelley@fsu.edu)

0886-6236/12/2011GB004155

absolute requirement for Co [*Sunda and Huntsman*, 1995; *Saito et al.*, 2002]. Given that *Prochlorochoccus* is thought to be the most abundant marine autotroph and thus accounts for a significant proportion of global photosynthesis [*Goericke and Welschmeyer*, 1993; *Campbell et al.*, 1994; *Partensky et al.*, 1999], there is a need to assess the potential role of Co in controlling the growth and distribution of this organism. In addition, there is emerging evidence that some forms of alkaline phosphatase (AP), a metalloenzyme that facilitates the acquisition of phosphorus (P) from the dissolved organic phosphorus (DOP) pool [*Cembella et al.*, 1982], may contain Co rather than Zn as a metal cofactor [*Plocke et al.*, 1962; *Gong et al.*, 2005]. Expression of AP is of particular importance in the North Atlantic Subtropical Gyre, where up to 30% of primary production may be supported by the DOP pool [*Mather et al.*, 2008]. *Jakuba et al.* [2008] have also provided evidence for important linkages in the biogeochemical cycles of Co, Zn and P in the phosphorus-poor surface waters of the Sargasso Sea. At present, however, the biogeochemical cycling of Co and the extent to which this trace element may influence the phytoplankton community in the surface ocean are not well understood.

[4] Cobalt and Fe share similarities in their marine biogeochemistry, in that the vertical distributions of both metals are strongly influenced by biological uptake, recycling, scavenging and remineralization [*Saito and Moffett*, 2002]. Vertical concentration profiles of dissolved Co and Fe can be considered to reflect a hybrid of 'nutrient-type' and 'scavenged-type' behavior [*Noble et al.*, 2008; *Boyd and Ellwood*, 2010]. Furthermore, dissolved Co and Fe share similar chemical speciation in seawater: both are present in the +3 oxidation state under oxic conditions, and both are strongly complexed by organic ligands. For example, *Ellwood and van den Berg* [2001] found that when Co-binding ligands were present in excess of total dissolved cobalt (dCo), all of the dCo was organically bound. Similarly, >99% of the total dissolved iron (dFe) in seawater has been shown to be complexed by organic ligands [*Gledhill and van den Berg*, 1994; *van den Berg*, 1995; *Rue and Bruland*, 1997].

[5] Dissolved Co concentrations in open ocean surface waters are extremely low (~4–120 pM [e.g., *Knauer et al.*, 1982; *Martin et al.*, 1987; *Saito et al.*, 2004]), with remote ocean regions tending toward the lower end of this range. In the Sargasso Sea, for instance, dCo concentrations < 20 pM are reported [*Jickells and Burton*, 1988; *Saito and Moffett*, 2002]. In the upper water column (at 42–44 m) at the Bermuda Atlantic Time series Study station (BATS, 31°N, 64°W), *Saito and Moffett* [2002] reported a significant depletion in dCo (annual mean 20 ± 10 pM) relative to concentrations below the euphotic zone (~30–40 pM). These workers observed no clear relationship between the summer maximum in aeolian dust deposition and surface dCo concentrations. In contrast, dFe shows clear evidence of significant aeolian input to the Sargasso Sea surface waters [*Wu and Boyle*, 2002; *Sedwick et al.*, 2005]. However, at a more northerly station in the North Atlantic Ocean (~40°N, 23°W), *Ellwood and van den Berg* [2001] have reported elevated dCo concentrations in the surface mixed layer (34 ± 3 pM at <40 m) relative to deeper waters in the photic zone (25 ± 4 pM at 65–165 m depth). This surface enrichment suggests a surface input, such as aerosol deposition, and/or variation in the rate of removal of dCo as a function of depth.

[6] Located in the western North Atlantic subtropical gyre, the Sargasso Sea is well situated for studying the impact of atmospheric deposition on the distribution of trace metals in the surface ocean, owing to the atmospheric and oceanographic time series observations that have been collected in the region over several decades. The atmospheric observations have shown that aerosols over Bermuda and the surrounding ocean region are typically dominated by air masses carrying North African mineral aerosols ('Saharan dust') during summer and early fall, whereas aerosols carried from North America, Asia and Europe are more abundant during the late fall through spring [e.g., *Duce and Hoffman*, 1976; *Chen and Duce*, 1983; *Arimoto et al.*, 1995, 2003; *Moody et al.*, 1995; *Huang et al.*, 1999; *Smirnov et al.*, 2002]. Recent work by *Sedwick et al.* [2007] and *Sholkovitz et al.* [2009] in the Bermuda region suggests that aerosols associated with North American air masses contain a greater proportion of anthropogenic combustion products, as well as Fe that is more water soluble relative to that delivered in Saharan dust.

[7] Mineral aerosols (dust) are thought to provide a major source of dFe to open ocean surface waters [*Duce and Tindale*, 1991; *Jickells et al.*, 2005], although the importance of aeolian deposition as a source of dCo to open ocean surface waters remains uncertain. If aerosol deposition does provide a significant source of Co to ocean surface waters, then differences in the fractional solubility of Co in aerosols of different composition/provenance [*Sedwick et al.*, 2007] and/or degree of atmospheric processing may be an important issue [*Mackie et al.*, 2005, 2006; *Baker et al.*, 2006; *Baker and Jickells*, 2006]. Here we attempt to gain insight into the sources and biogeochemical cycling of dissolved Co in the surface ocean, by examining trace metal data obtained for water column samples, underway surface water samples and aerosol samples collected along a meridional transect of the Sargasso Sea to the south of Bermuda in June 2008.

2. Sampling and Analysis

2.1. Study Area

[8] Samples were collected aboard the RV *Atlantic Explorer* during the *FeAST*-6 cruise, which included a meridional transect of the Sargasso Sea from the BATS region near 31°N south to ~24°N, over the period 5–18 June 2008. In terms of the flux and source of aerosols to the Sargasso Sea, June is a transitional month characterized by large variations in aerosol Fe loading and aerosol provenance (Saharan versus non-Saharan) [*Sholkovitz et al.*, 2009]. Later in the summer (July–September), Saharan dust typically dominates the mineral aerosol, with dust loadings generally higher than in preceding months [*Arimoto et al.*, 1995; *Huang et al.*, 1999; *Gao et al.*, 2001; *Sholkovitz et al.*, 2009]. The *FeAST*-6 cruise track (Figure 1a) was chosen to sample surface waters along a north-to-south gradient of increasing aerosol deposition [*Jickells et al.*, 2005], and to include water column sampling stations that were located both within and between mesoscale eddies, which were identified using sea level altimetry (Figure 1b). Information on the location and mesoscale circulation associated with each water column station sampled during the cruise is provided in Table 1.

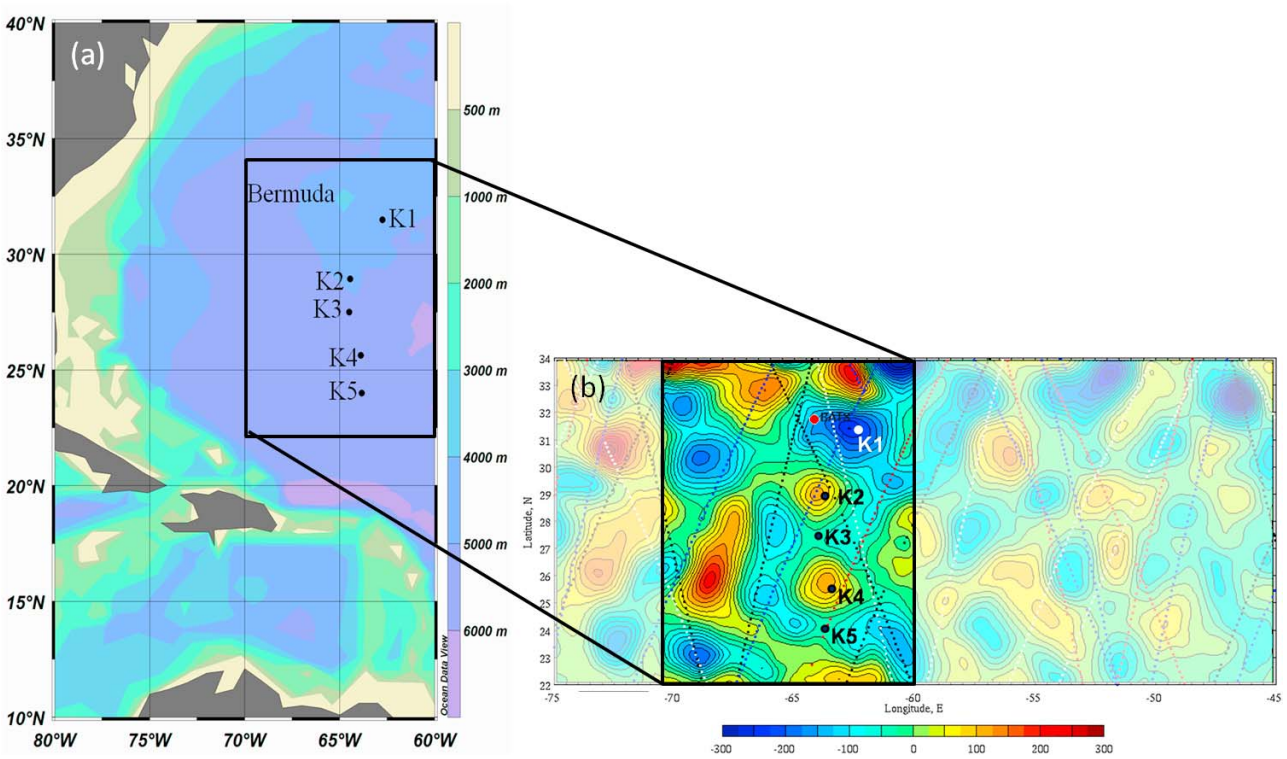

Figure 1. (a) *FeAST*-6 cruise track (June 2008) in the Sargasso Sea showing, from north to south, stations K1–K5 and (b) sea level altimetry analysis of the Sargasso Sea for 13 June 2008, showing location of trace metal water column sampling stations.

2.2. Seawater Sample Collection and Treatment

2.2.1. Water Column Samples

[9] Water column samples were collected for trace metal analysis from five stations (K1–K5) along the north–south transect (Figure 1 and Table 1). Samples were collected in modified 5 L Teflon-lined external closure Niskin-X samplers (General Oceanics Inc.) deployed on a Kevlar line [*Sedwick et al.*, 2005]. The surface seawater (0–1 m depth) samples for the water column profiles were collected in 1 L wide-mouth low density polyethylene bottles (LDPE, Nalgene) mounted on the end of a ~5 m bamboo pole, which was extended from the ship's stern for sample collection while backing slowly into the wind. Upon recovery, seawater samples were filtered inside a shipboard Class-100 clean container laboratory, through a 0.4 μm pore Supor Acropak filter capsule (Pall Corp.) that was pre-rinsed with ~5 L of ultrapure deioinized water (>18 MΩ cm, Barnstead Nanopure) followed by several hundred mL of each sample (Niskin-X samples), or through 0.4 μm pore Poretics polycarbonate membrane filters (surface sample only) mounted in a Savillex Teflon PFA filtering assembly [*Sedwick et al.*, 2005]. The filtered seawater samples were acidified to 0.024 M with ultrapure HCl (SpA Romil for Al and Co analysis; Seastar Baseline for Fe analysis) prior to analysis, and stored in rigorously acid-cleaned Nalgene LDPE bottles [*Sedwick et al.*, 2005; *Shelley et al.*, 2010].

2.2.2. Underway Surface Samples

[10] To investigate lateral variations in the surface concentrations of dissolved Co, Fe and Al, near-surface seawater samples were collected during four transects between the five water column sampling stations. Seawater was pumped from ~5 m depth directly into a shipboard Class-100 'clean bubble' using a trace-metal clean towfish sampler [*Bruland et al.*, 2005]. During these transects, water samples were collected every hour, thereby providing near-surface water samples at spacings of ~12 km. The underway seawater samples were filtered in-line through a 0.4 μm pore Supor Acropak filter capsule (Pall Corp.), then acidified to ~0.024 M with ultrapure HCl and stored in LDPE bottles, as described for the water column samples.

2.2.3. Determination of Trace Metals in Seawater Samples

[11] Both dCo and dFe were determined by flow injection analysis with in-line preconcentration. For the determination of dCo, the flow injection manifold was coupled with a photomultiplier tube and dCo was determined in UV-irradiated samples by means of chemiluminescence, as described by *Shelley et al.* [2010]. Dissolved Fe was determined by flow injection analysis with spectrophotometric detection modified from the method of *Measures et al.* [1995], as described

Table 1. Details of Water Column Trace Metal Sampling Stations Occupied During *FeAST*-6

Station	Date	Lat (°N)	Long (°W)	Mesoscale Context
K1	06/06/2008	31.48	62.75	Cyclonic eddy
K2	06/09/2008	28.93	64.44	Anticyclonic eddy
K3	06/10/2008	27.50	64.50	Between eddies
K4	06/13/2008	25.63	63.88	Anticyclonic eddy
K5	06/14/2008	24.00	63.88	Between eddies

by *Sedwick et al.* [2008]. Dissolved Al was determined by flow injection analysis using micelle-enhanced fluorimetric detection using Brij-35 as the surfactant instead of Triton-X 100 [*Resing and Measures*, 1994; *Brown and Bruland*, 2008].

[12] Accuracy of the analytical methods used for the determination of dCo, dFe and dAl was assessed by analysis of reference seawater samples from the SAFe and GEOTRACES programs (all concentrations reported are ±1 sd). For dCo, the method used in this study yielded 40.9 ± 2.6 pM (n = 12) for SAFe reference seawater D2, compared with the consensus value of 45.4 ± 3.8 pM and, 73 ± 3 pM (n = 3) for the GEOTRACES reference sample GD, compared with the consensus value of 65 ± 8 pM. For dFe, the method used in this study yielded 0.11 ± 0.01 nM (n = 15) and 0.97 ± 0.06 nM (n = 14) for SAFe reference seawater S1 and D2, compared with consensus values of 0.090 ± 0.007 nM and 0.90 ± 0.02 nM respectively. For dAl, the method used in this study yielded 28.8 ± 2.7 nM (n = 14) and 17.3 ± 2.5 nM (n = 14) for GEOTRACES reference seawater GS and GD, compared with consensus values of 27.5 ± 0.2 nM and 17.7 ± 1 nM respectively (consensus values for the SAFe and GEOTRACES seawater are listed at http://www.geotraces.org/news/news/1-news-/329-updated-consensus-values-for-the-safe-and-north-atlantic-geotraces-reference-seawater-samples.

2.3. Aerosol Sample Collection and Treatment

[13] Aerosol samples were collected at sea during the *FeAST*-6 cruise using low volume pumps (airflow rate ~2 m^3 h^{-1}) to pull air through acid-cleaned 47 mm diameter filter membranes mounted in downward-facing filter heads fitted with polyethylene rain shields [*Véron and Church*, 1997; *Sedwick et al.*, 2007]. The filter heads were positioned on a 7 m high sampling tower erected forward of the ship's bridge. Samples were collected while the ship was slowly underway heading into the wind, over periods of ~6–12 h. Two filter types were deployed in parallel: Millipore HA filters (0.45 μm nominal cutoff size) for the analysis of bulk aerosol composition, and Poretics polycarbonate membranes (0.4 μm pore size) for aerosol leaching experiments (see below).

2.3.1. Processing and Analysis of Aerosol Samples

[14] For determinations of bulk aerosol composition, the aerosol-laden Millipore HA filter halves were treated with a 1:3 (v/v) mixture of 48% (w/w) hydrofluoric acid solution and 70% (w/w) nitric acid solution at 80°C for one day in the laboratory at UDE. Any filter residue was removed following dissolution of the aerosol particles, then the solution was heated to dryness. The digestion residue was re-dissolved in 1 N nitric acid. Total Co, Fe and Al were determined by inductively coupled plasma mass spectrometry (ICP-MS; Finnegan Element2). It is assumed that the Co, Fe and Al measured in the aerosol digest solutions account for both the labile and refractory fractions of these elements in the bulk aerosol, thus allowing calculation of 'total aerosol' concentrations in units of pmol m^{-3} air (for total Co) or nmol m^{-3} air (for total Fe and total Al), using the total volume of air that passed through each aerosol filter sample.

[15] The percent fractional solubility of aerosol Co and Fe (%Co_S or %Fe_S) was estimated using a modification of the flow-through deionized water leaching protocol of *Buck et al.* [2006]. In this study, 250 mL of ultrapure deionized water (>18 MΩ cm resistivity, pH ~ 5.5, Barnstead Nanopure) was rapidly passed through an aerosol-laden polycarbonate filter membrane held in a Savillex Teflon PFA filtering assembly [*Sedwick et al.*, 2007]. The aerosol leaches were conducted under a Class-100 laminar flow hood within 6 h of sample collection. The filtrate (leachate) was immediately transferred into a 125 mL LDPE bottle and acidified to ~0.024 M with Seastar Baseline ultrapure hydrochloric acid. Dissolved Co and Fe were subsequently determined in the leachate solutions by ICP-MS and by flow injection analysis, respectively, as described by *Sholkovitz et al.* [2009]. Blank solutions (0.0051 μg L^{-1} dCo) were prepared by passing 250 mL of deionized water over clean polycarbonate filter membranes that had been mounted on the shipboard sampling tower without running the pumps. Fractional solubility is operationally defined as the aerosol concentration of soluble aerosol Co or Fe as calculated from dCo and dFe concentrations in the leachate solutions, expressed as a percentage of the total aerosol concentration of Co or Fe as calculated from analysis of the filter digest solutions [*Sedwick et al.*, 2007].

2.3.2. Air Mass Back Trajectories

[16] Seven day air mass back trajectories were simulated for each sampling location using the NOAA Air Resources Laboratory Hybrid Single-Particle Lagrangian Integrated Trajectory (HYSPLIT) model (see R. R. Draxler and G. D. Rolph, HYSPLIT—Hybrid Single-Particle Lagrangian Integrated Trajectory model, Air Resources Laboratory, NOAA, Silver Spring, Maryland, 2010, available at http://ready.arl.noaa.gov/HYSPLIT.php; G. D. Rolph, Real-time Environmental Applications and Display System (READY) Web site, Air Resources Laboratory, NOAA, Silver Spring, Maryland, 2010, available at http://ready.arl.noaa.gov). Arrival heights of 200 m and 1500 m were selected; the 1500 m arrival height was chosen to include the Saharan air layer, which typically delivers Saharan dust to the American continent in summer at altitudes of ~1.5–6 km [*Prospero and Carlson*, 1972; *Prospero et al.*, 1981], whereas the 200 m arrival height was chosen to represent aerosols carried within the marine boundary layer.

2.4. Enumeration of Phytoplankton Groups

[17] Three groups of picophytoplankton were enumerated using a FACSort flow cytometer (Becton Dickinson, Oxford, U.K.). For the flow cytometry analyses, 1.8 mL whole seawater samples were fixed with 1% paraformaldehyde and incubated at 4°C for 24 h before freezing and storage at −80°C. *Prochlorococcus*, *Synechococcus* and picoeukaryote cells were identified and enumerated using group-specific side scatter, along with orange (585 ± 21 nm) and red (>650 nm) autofluorescence properties [*Olson et al.*, 1993]. Multifluorescent beads (0.5 μm) were added to all samples at known concentrations to enable enumeration using syringe pumped flow cytometry [*Zubkov and Burkill*, 2006].

3. Results and Discussion

3.1. Hydrographic and Biogeochemical Observations

[18] In the Sargasso Sea, the region between 25°N and 32°N represents a zone of transition between permanently stratified oligotrophic waters of the subtropical convergence

zone in the south to seasonally stratified oligotrophic waters in the north [*Steinberg et al.*, 2001]. In the BATS region near 31°N, convective mixing to depths of 150–300 m during late fall through early spring replenishes surface waters with macronutrients, which are subsequently depleted to nanomolar concentrations between April and October, when the surface mixed layer depth shoals to depths of less than 20 m [*Steinberg et al.*, 2001]. Net surface flow in our study region is dominated by southwesterly geostrophic circulation, whereas westerly propagating mescoscale eddies tend to dominate surface ocean circulation over sub-seasonal timescales [*Siegel et al.*, 1999; *Steinberg et al.*, 2001; *McGillicuddy et al.*, 2007].

[19] Hydrographic data (temperature, salinity and in situ fluorescence) from the *FeAST*-6 water column sampling stations are shown in Figure 2. The surface mixed layer depth (MLD) was ∼10 m along the entire transect, as is typical of this ocean region in summer. Dissolved nitrate and phosphate were depleted to concentrations of <50 nM to depths of ∼100–150 m at each of the water column sampling stations. In addition, a subsurface chlorophyll maximum was observed at a depth of ∼150 m along the cruise track (Figure 2). Another notable feature observed at each station was a significant freshening in the surface mixed layer, indicating an excess of precipitation over evaporation in our study region during the months prior to the cruise. This interpretation is supported by rainfall data from the Tudor Hill atmospheric observatory and the Bermuda Weather Service, which reveal above-average precipitation during April and May 2008, immediately prior to the cruise.

3.2. Surface Transects

[20] Surface samples were collected along the cruise track to investigate lateral variability in dCo, dFe and dAl concentrations in surface waters of our study region. Figure 3 shows the surface distributions of dCo, dFe and dAl from ∼31°N to ∼24°N. All three trace metals displayed significant lateral variations in surface concentrations, both within and between the four underway transects (dCo = 18–63 pM, dFe = 0.3–1.6 nM, dAl = 14–42 nM). Surface dFe and dAl concentrations were lowest at the northern end of the transect (0.3–0.4 nM dFe and 14–27 nM dAl), and increased toward the south, reaching maximum concentrations of 1.2–1.6 nM dFe at 24–26°N, and 38–42 nM dAl at 26–27°N (Figure 3). In contrast, surface dCo concentrations showed no clear latitudinal trend; concentrations ranged from 18 to 63 pM, with the majority of samples close to the mean dCo value of 42 pM.

[21] The measured range of surface dFe and dAl concentrations are in general agreement with values previously reported for surface waters in the Sargasso Sea [*Measures et al.*, 1986; *Jickells et al.*, 1994; *Wu and Boyle*, 2002; *Sedwick et al.*, 2005]. In regions remote from mineral aerosol sources, surface dFe and dAl concentrations are typically less than ∼0.2 nM and ∼1 nM, respectively [*Jickells et al.*, 1994; *Johnson et al.*, 1997; *Measures and Vink*, 2000; *Moore and Braucher*, 2008]. The substantially higher surface dFe and dAl concentrations that we report are clearly indicative of dust deposition, given the significant correlation between surface dFe and dAl values (r^2 = 0.63, Figure 3), and the general north-to-south concentration increase, which follows the expected latitudinal gradient in average dust deposition to the North Atlantic [*Arimoto et al.*, 1995; *Jickells et al.*, 2005]. The surface dAl concentrations (38–42 nM) that we measured are significantly higher than values reported for similar latitudes along the CLIVAR A16N section (12–24 nM), located to the east of our cruise track [*Measures et al.*, 2008]. This observation is consistent with the suggestion that atmospheric circulation results in higher surface concentrations of dAl in the western versus eastern basin of the North Atlantic at these latitudes, despite the proximity of the eastern basin to the major soil dust sources in North Africa [*Measures and Brown*, 1996; *Jickells et al.*, 2005; *Measures et al.*, 2008].

[22] In a larger study of the subtropical and tropical Atlantic Ocean, *Bergquist and Boyle* [2006] reported that the gradient in surface dFe concentrations reflected dust deposition trends, but was not proportional to the surface dAl gradient nor estimated aeolian input fluxes. Between the North and South Atlantic, dAl concentrations decreased by a factor of ∼5, whereas dFe concentrations decreased by only ∼2-fold [*Bergquist and Boyle*, 2006; *Vink and Measures*, 2001]. *Bergquist and Boyle* [2006] have suggested that this reflects the short residence time of dFe in the surface ocean, relative to dAl, as well as the generally low solubility of iron in seawater, which may limit the dissolution of aerosol iron. In addition, *Sedwick et al.* [2007] have proposed that latitudinal differences in the fractional solubility of aerosol iron may serve to decouple surface ocean dFe concentrations from total dust deposition, such that the impact of Saharan dust deposition is limited by the inherently low fractional solubility of iron in North African mineral aerosols.

[23] Interestingly, our data show that surface dFe and dAl concentrations both increase by a factor of ∼2–3 from north to south, which is approximately proportional to the corresponding latitudinal gradient in average dust deposition [*Jickells et al.*, 2005]. Following the reasoning of *Bergquist and Boyle* [2006], these observations may suggest that dissolved Fe and Al have similar residence times in surface waters of the Sargasso Sea, at least prior to the seasonal maximum in Saharan dust deposition during July and August [*Huang et al.*, 1999; *Arimoto et al.*, 2003]. Alternately, our observations may reflect the high fractional solubility of iron in aerosols that are deposited to the Sargasso Sea during spring and early summer [*Sedwick et al.*, 2007; *Sholkovitz et al.*, 2009], compared with the aerosols that impact surface waters of the larger Atlantic region. Also noteworthy is the significant sub-mesoscale variability that we observed in surface dFe, dAl and, in particular, dCo concentrations, which may reflect the impact of surface circulation and/or small-scale lateral variability in atmospheric input (e.g., due to patchy wet deposition) or biological removal.

[24] With regard to surface dCo concentrations, the absence of a clear latitudinal increase may be interpreted to suggest that atmospheric deposition is not a major source of dCo to surface waters in the Sargasso Sea, at least not during the spring and early summer. Alternatively, the effective residence time of dCo may be short enough to obscure the relationship between dust deposition and surface ocean concentration. Data from the BATS region provide some support for the latter hypothesis, with estimated upper water column (<100 m depth) residence times of 117 days for dCo [*Saito and Moffett*, 2002] versus 214–291 days for dFe

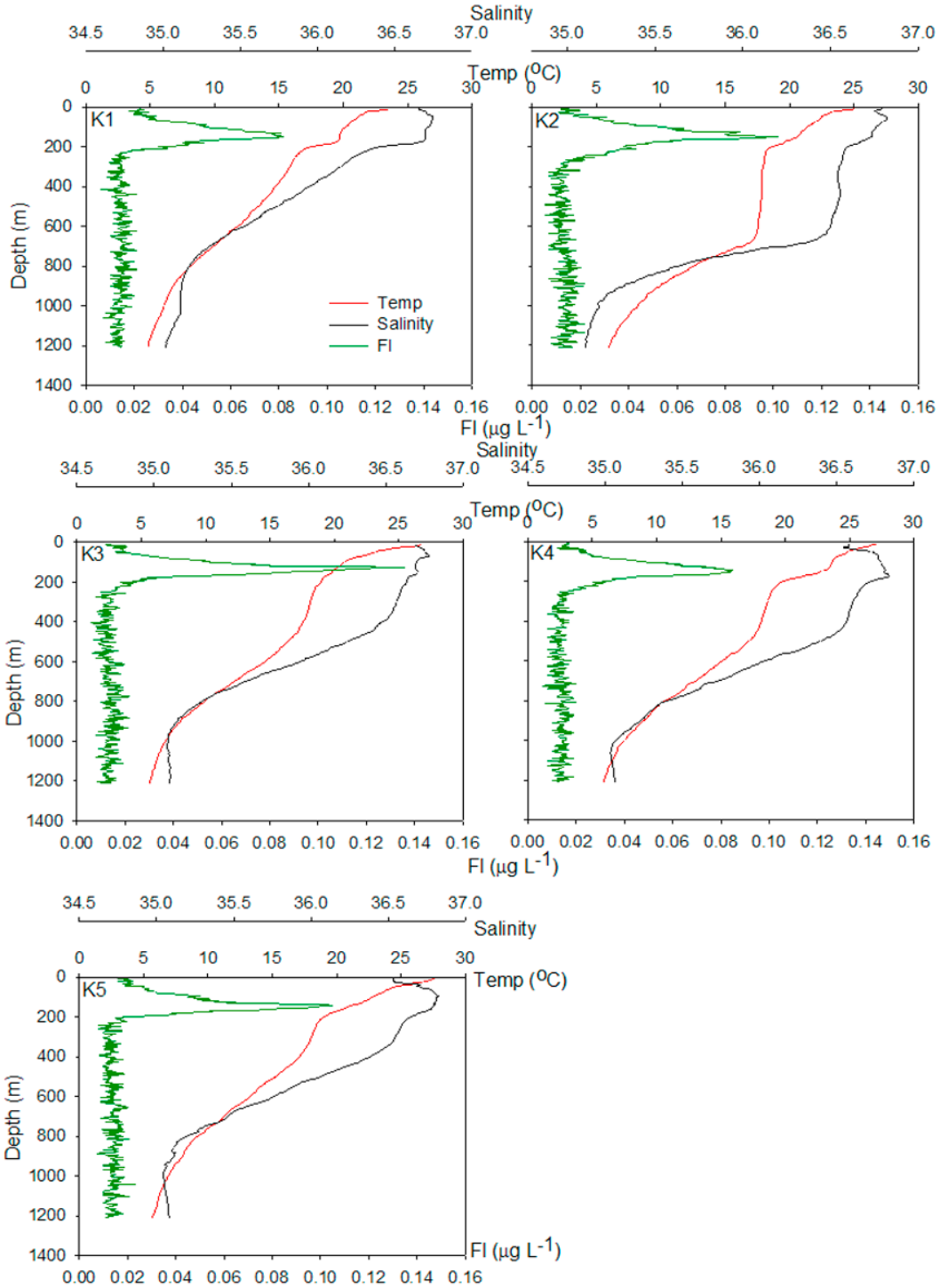

Figure 2. Vertical profiles of temperature (°C), salinity and in situ chlorophyll-*a* fluorescence (μg L^{-1}) from CTD-rosette casts at stations K1–K5.

[*Jickells*, 1999]. Further, the fact that we observed a mean surface dCo concentration (42 pM) that is significantly higher than the annual average concentration for the upper water column in the BATS region (20 $\pm$ 10 pM) [*Jickells and Burton*, 1988; *Saito and Moffett*, 2002] would seem to imply a significant aeolian input of dCo to our study region. In addition, we note that the fractional solubility of aerosol Co, which may vary with latitude, could conceivably decouple surface dCo concentrations from the magnitude of dust deposition to the ocean. We explore some of these possibilities in the following sections.

3.3. Fractional Solubility of Aerosol Cobalt and Iron

[25] To estimate the dry deposition of dCo to our study region during the cruise period, ship-board aerosol samples were collected between the water column stations. The

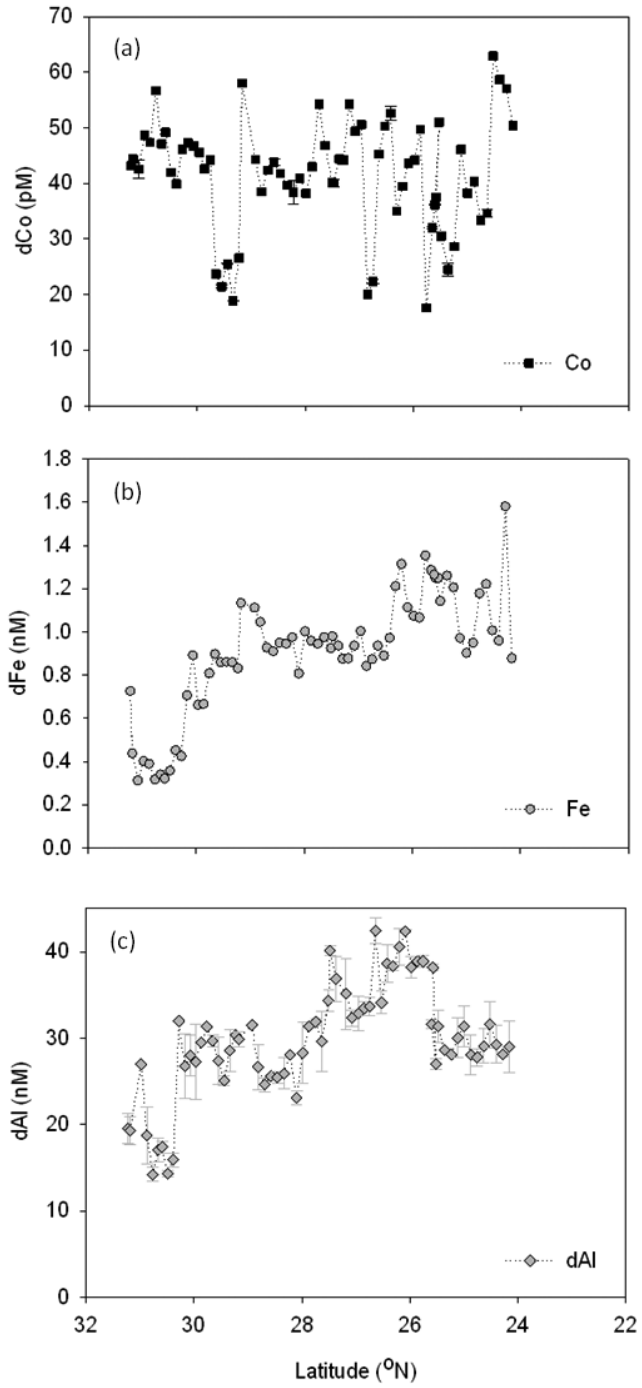

Figure 3. Surface concentrations of (a) dCo, (b) dFe, and (c) dAl along the *FeAST*-6 transect from ~31°N to ~24°N ($\pm 1\sigma$ where shown).

total aerosol Co loading in the samples ranged from 5.4 to 11.0 pg Co m^{-3}. The total aerosol Co loadings can be used to estimate the dry deposition flux of total aerosol Co (total Co F_{dry}) using the following equation [*Arimoto et al.*, 1985]:

$$\text{total Co } F_{dry} = C_a \times V_d \quad (1)$$

where C_a is the total aerosol Co loading and V_d is the dry deposition velocity of the cobalt-bearing aerosol particles, for which we will assume a constant value of 0.01 m s^{-1} [*Arimoto et al.*, 1985; *Tian et al.*, 2008]. This yields estimates of air-sea dry deposition fluxes of 4.7–9.5 ng Co m^{-2} d^{-1} along our cruise track (Table 2a).

[26] Our estimates of the fractional solubility of aerosol Co based on deionized water leaches suggest that most (75–100%) of the Co delivered to the surface ocean during the *FeAST*-6 cruise was readily 'soluble'. These values are substantially higher than corresponding estimates of the fractional solubility of aerosol Fe (5–45%) in the same samples. Although the solubility of Co in different types of dust has been examined in the laboratory [e.g., *Thuróczy et al.*, 2010], there has been little research on the fractional solubility of Co in marine aerosols. The estimates from this study (Tables 2a and 2b) suggest a much greater fractional solubility for aerosol Co in our study region (75–100%) than for coal fly ash (0.78%) or Cape Verde loess (0.14%) reported by *Thuróczy et al.* [2010]. This suggests that aerosols sampled during our cruise may contain Co that is inherently more soluble than that in coal ash or soil dust, and/or that long range atmospheric processing may increase the solubility of aerosol Co in transit from its source regions.

[27] In this study the highest fractional solubility of Co (~100%) was associated with the lowest aerosol Fe loading (10 ng m^{-3}). Aerosol iron solubility in the BATS region has been found to vary inversely as a function of the total Fe loading on the bulk aerosol, with differences in the relative solubility and total aerosol Fe loadings attributed to the origin and composition of the aerosol particles; specifically, low aerosol Fe loadings and relatively high aerosol Fe solubilities were associated with air masses carried from North America or Europe [*Sedwick et al.*, 2007]. Our data from shipboard aerosol samples suggest that the aerosols collected during *FeAST*-6 contained a significant proportion of non-Saharan particles. Indeed, air mass back trajectory simulations indicate a predominantly North American origin for aerosols sampled during the cruise (Figure 4).

[28] By multiplying our estimates of the dry deposition flux of total Co by our corresponding estimates of the fractional solubility of aerosol Co (%Co_S), the deposition flux of 'soluble' aerosol Co (soluble Co F_{dry}) can be estimated according to:

$$\text{solubleCo } F_{dry} = (C_a \times V_d) \times (\%Co_s/100) \quad (2)$$

The calculated range of soluble Co F_{dry} in Table 2a (47–155 pmol dCo m^{-2} d^{-1}) suggests that between 0.4 and 1.4 pM of dCo could be supplied to the surface mixed layer over a six month period of stratification, assuming a mixed layer depth of ~20 m. This estimated atmospheric input is low, relative to the observed surface concentrations of ~20–60 pM, and is therefore unlikely to contribute to the lateral variability that we observed in surface dCo concentrations. However, considering that the similarly estimated dry deposition flux of Fe during our study period was low (1–4 μg Fe m^{-2} d^{-1}) compared with the annual range estimated for Bermuda (0.1–10,000 μg m^{-2} d^{-1}) [*Sholkovitz et al.*, 2009], our estimate of the mean dry deposition of soluble Co during the *FeAST*-6 cruise (0.006 μg m^{-2} d^{-1}) is likely to represent a very conservative lower limit for this flux to the Sargasso Sea during the summer months. A similar calculation of the dry deposition of soluble Fe during our

Table 2a. Aerosol Co Fluxes and Fractional Solubility During *FeAST*-6 Cruise[a]

Date Aerosol Collected	Total Aerosol Co Loading (μg Co/m^3 air)	Deposition Velocity (m/s)	Total Co Flux$_{dry}$ (μg/m^2/d)	%Co$_S$	Soluble Co Flux$_{dry}$ (μg/m^2/d)	Soluble Co Flux$_{dry}$ (pmol/m^2/d)
9 June 2008	0.00000544	0.01	0.00470	93	0.00435	74
10 June 2008	0.0000106	0.01	0.00914	100	0.00914	155
12 June 2008	0.0000110	0.01	0.00952	75	0.00712	121
14 June 2008	0.00000401	0.01	0.00346	79	0.00274	47
16 June 2008	0.0000105	0.01	0.00907	78	0.00712	121

[a]The *FeAST*-6 cruise was characterized by low dust loadings. Note that the calculated fractional solubility for one sample (calculated at 115%) has been corrected to the maximum possible value of 100%; this is likely to be an analytical artifact reflecting the very low concentrations of Co (5–15 pg Co m^{-3} air) in the bulk aerosol (*c.f.* 10–28 ng Fe m^{-3} air).

cruise (Table 2b) yields an estimated accumulation of 0.2–0.7 nM dFe in a 20-m surface mixed layer over six months.

[29] Here it is informative to compare our atmospheric deposition estimates with results from the *FeATMISS*-1 cruise, which took place in the Sargasso Sea from July 22–August 6, 2003, during the peak of the Sarahan dust season [*Sedwick et al.*, 2005, 2007]. The estimated mean dry deposition of Fe during the *FeATMISS*-1 cruise (1040 μg Fe m^{-2} d^{-1}; Table 3b) is more than two orders of magnitude greater than the flux estimated during our *FeAST*-6 cruise. Similarly, the total aerosol loadings of Co during the *FeATMISS*-1 cruise yield estimates of 0.35–0.89 μg m^{-2} d^{-1} for the total dry deposition flux of Co (Table 3a; E. R. Sholkovitz, unpublished data, 2010). Interestingly, the estimated fractional solubility of Co in the *FeATMISS*-1 aerosols ranges from 8 to 10%, suggesting an inverse relationship between the fractional solubility of aerosol Co and total aerosol loading, as has been reported for aerosol Fe, V, Ni and Cu [*Sedwick et al.*, 2007; *Sholkovitz et al.*, 2009, 2010]. These fractional solubility values yield estimates of the dry deposition of 'soluble' Co in the range of 590–1540 pmol dCo m^{-2} d^{-1} (Table 3a; E. R. Sholkovitz, unpublished data, 2010). These values are an order of magnitude greater than the corresponding flux estimates from our *FeAST*-6 cruise, and could increase the dCo concentration in a 20-m mixed layer by as much as 5–14 pM over a period of six months, thus accounting for a significant fraction of the surface dCo inventory.

[30] The ~10-fold difference between estimates of the atmospheric deposition of 'soluble' Co from the *FeAST*-6 and *FeATMISS*-1 cruises implies a significant temporal variability in the aeolian input of dissolved Co to the Sargasso Sea, such that 'snapshots' of atmospheric deposition based on aerosols sampled during short research cruises are unlikely to provide robust estimates of seasonal-scale atmospheric inputs. Indeed, it is unclear whether the soluble Co deposition estimates from the *FeAST*-6 and *FeATMISS*-1 cruises reflect seasonal differences in atmospheric inputs during the early summer and late summer, respectively, or stochastic variations in atmospheric deposition. The latter possibility merits some consideration, given the significant lateral variations in surface dCo concentrations observed along our cruise track (Figure 3a). In this regard, time series data from aerosol samples collected at island sites may provide useful information, as is implied by the excellent agreement between aerosol iron loadings based on aerosol samples collected on Bermuda and at the Bermuda Testbed Mooring [*Sholkovitz and Sedwick*, 2006].

[31] An additional and potentially important atmospheric input of cobalt to surface waters in our study region is via wet deposition. Due to the relatively low pH of rainwater, and the strong pH dependence of transition metal solubility [*Stumm and Morgan*, 1996], wet deposition may constitute a major source of trace metals to the open ocean [*Helmers and Schrems*, 1995; *Jickells*, 1999; *Baker et al.*, 2007]. The estimates of atmospheric Co deposition that are discussed above do not include wet deposition, since no significant rain events were sampled during the *FeAST*-6 cruise. However, there had clearly been substantial rainfall in the months prior to the cruise, as discussed in section 3.1. For Fe, wet deposition is thought to account for <30% of the total atmospheric deposition flux to Bermuda [*Tian et al.*, 2008; T. M. Church, unpublished data, 2010]. In contrast, limited data from the analysis of aerosols and rainwater collected on Bermuda suggests that the atmospheric deposition of Co may be dominated (>80%) by wet deposition (T. M. Church, unpublished data, 2010). Assuming a similar proportion of wet deposition of soluble Co to our study region (i.e., 80% wet, 20% dry) yields a wet deposition flux of 190–620 pmol dCo m^{-2} d^{-1}, based on the dCo dry deposition flux estimated from the *FeAST*-6 aerosol samples. This

Table 2b. Aerosol Fe Fluxes and Fractional Solubility During *FeAST*-6 Cruise[a]

Date Aerosol Collected	Total Aerosol Fe Loading (μg Fe/m^3 air)	Deposition Velocity (m/s)	Total Fe Flux$_{dry}$ (μg/m^2/d)	%Fe$_S$	Soluble Fe Flux$_{dry}$ (μg/m^2/d)	Soluble Fe Flux$_{dry}$ (nmol/m^2/d)
9 June 2008	0.0115	0.01	9.93	9	0.865	15.5
10 June 2008	0.0105	0.01	9.07	45	4.06	72.7
12 June 2008	0.0133	0.01	11.5	36	4.15	74.3
14 June 2008	0.0276	0.01	23.9	5	1.21	21.7
16 June 2008	0.0163	0.01	14.1	10	1.38	24.8

[a]The *FeAST*-6 cruise was characterized by low dust loadings.

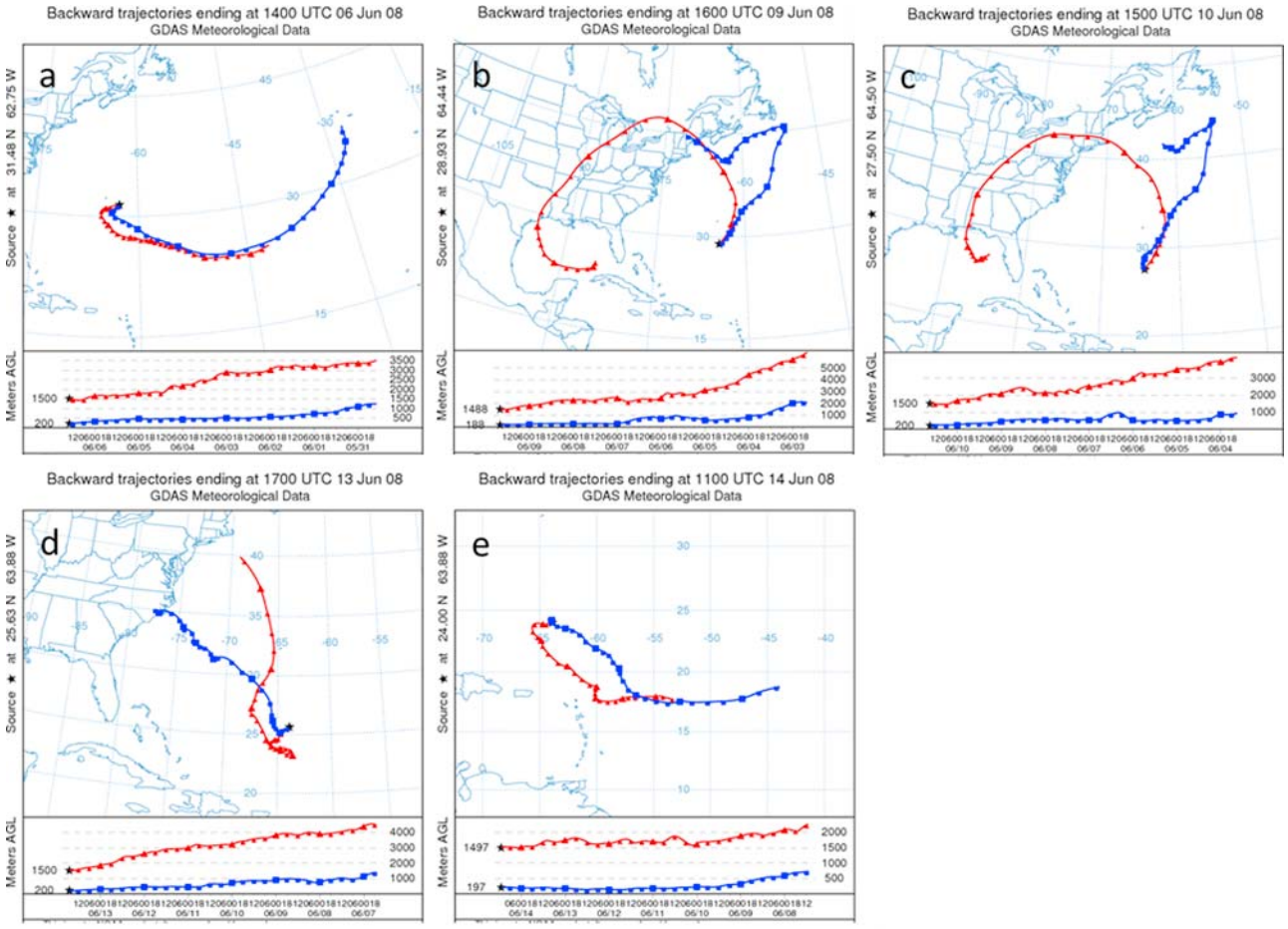

Figure 4. Seven day air mass back trajectory simulations (HYSPLIT model) for stations during *FeAST*-6 showing (a) K1, Atlantic maritime (a 10 day back trajectory indicated no contact with major landmasses within the modeled period); (b) K2, North American; (c) K3, North American; (d) K4, North American; and (e) K5, Atlantic maritime (a 10 day back trajectory indicated no contact with major landmasses within the modeled period) end-members.

translates to a rainwater input of 1.6–5.6 pM dCo to a 20-m thick mixed layer over six months, and thus a small but potentially significant fraction of the surface dCo inventory. Moreover, the inherently patchy, episodic nature of rain events may explain some of the lateral variability that is seen in surface dCo concentrations (Figure 3a).

3.4. Factors Influencing the Distribution of Cobalt in the Water Column

[32] A comparison of the vertical distributions of dCo, dFe and dAl (Figures 5 and 6) reveal clear meridional trends for all three metals, as well as some inter-station differences that appear to reflect the influence of mesoscale eddies. In examining these data, it is important to consider that our north-to-south cruise transect (from K1 through K5) traverses significant gradients in both physical structure and aeolian deposition. At the northern end of the transect, near station BATS, the water column is seasonally mixed to several hundred meters depth, whereas the water column is permanently stratified at the southern end of the transect [*Steinberg et al.*, 2001]. With regard to aeolian inputs, there is a several-fold increase in atmospheric dust loadings between the northern and southern ends of our cruise track, with a greater seasonality of dust deposition observed in the

Table 3a. Aerosol Co and Fluxes and Fractional Solubilities During *FeATMISS*-1 Cruise[a]

Date Aerosol Collected	Total Aerosol Co Loading (μg Co/m^3 air)	Deposition Velocity (m/s)	Total Co Flux$_{dry}$ (μg/m^2/d)	%Co$_S$	Soluble Co Flux$_{dry}$ (μg/m^2/d)	Soluble Co Flux$_{dry}$ (pmol/m^2/d)
01–02 Aug 2003	0.00104	0.01	0.899	10	0.0908	1540
03–04 Aug 2003	0.00100	0.01	0.864	8	0.0731	1240
04–05 Aug 2003	0.00041	0.01	0.354	10	0.0350	593

[a]The *FeATMISS*-1 cruise was characterized by high loadings of Saharan dust.

Table 3b. Aerosol Fe Fluxes and Fractional Solubilities During *FeATMISS*-1 Cruise[a]

Date Aerosol Collected	Total Aerosol Fe Loading (μg Fe/m^3 air)	Deposition Velocity (m/s)	Total Fe Flux$_{dry}$ (μg/m^2/d)	%Fe$_S$	Soluble Fe Flux$_{dry}$ (μg/m^2/d)	Soluble Fe Flux$_{dry}$ (nmol/m^2/d)
01–02 Aug 2003	1.56	0.01	1350	1.10	14.9	266
03–04 Aug 2003	1.55	0.01	1341	0.44	5.91	106
04–05 Aug 2003	0.495	0.01	428	1.10	4.70	84.2

[a]The *FeATMISS*-1 cruise was characterized by high loadings of Saharan dust.

Bermuda region [*Arimoto et al.*, 2003; *Jickells et al.*, 2005]. The latter point is important with regard to this data set, in that our water column sampling took place in early June, prior to the seasonal maximum in dust loading toward the northern end of the cruise transect.

[33] The influence of atmospheric deposition is most clearly displayed in the vertical distribution of dissolved aluminum, which is thought to have a strong aeolian source, limited biological involvement, and a long residence time relative to dissolved Fe and Co in the ocean [*Measures et al.*, 1986; *Orians and Bruland*, 1986; *Jickells*, 1999; *Measures and Vink*, 2000; *Saito and Moffett*, 2002]. This and the 'scavenged-type' behavior of dAl in the oceanic water column [*Measures et al.*, 1986] are clearly evident in the vertical concentration profiles from the *FeAST*-6 cruise (Figures 5a and 6a), with surface enrichment that increased from north to south (12–35 nM), and a general decrease in sub-surface waters to minimum concentrations at the greatest sampling depth of 1000 m (0.4–8 nM). Such scavenged-type profiles are characteristic of dAl in both the North Atlantic and North

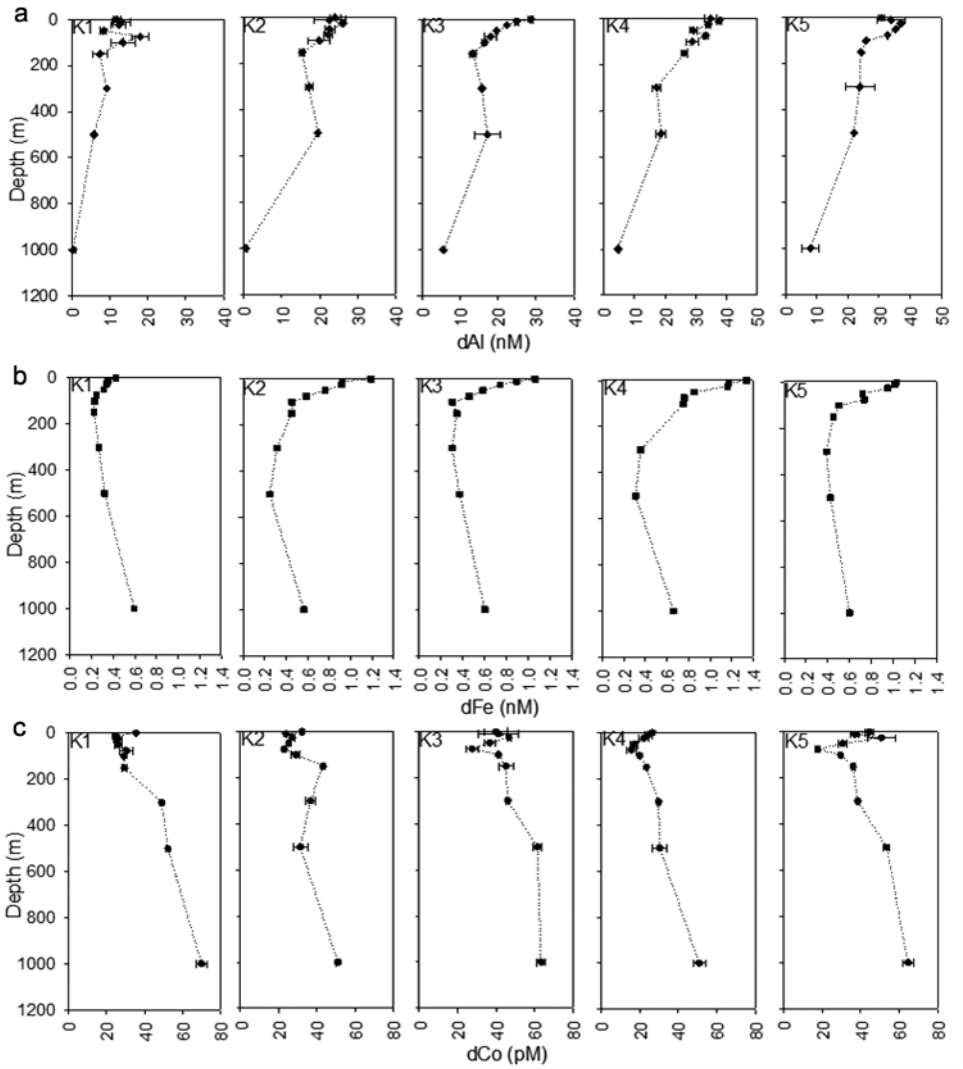

Figure 5. Vertical profiles of (a) dAl (nM), (b) dFe (nM), and (c) dCo (pM) at stations K1–K5 ($\pm 1\sigma$ where shown).

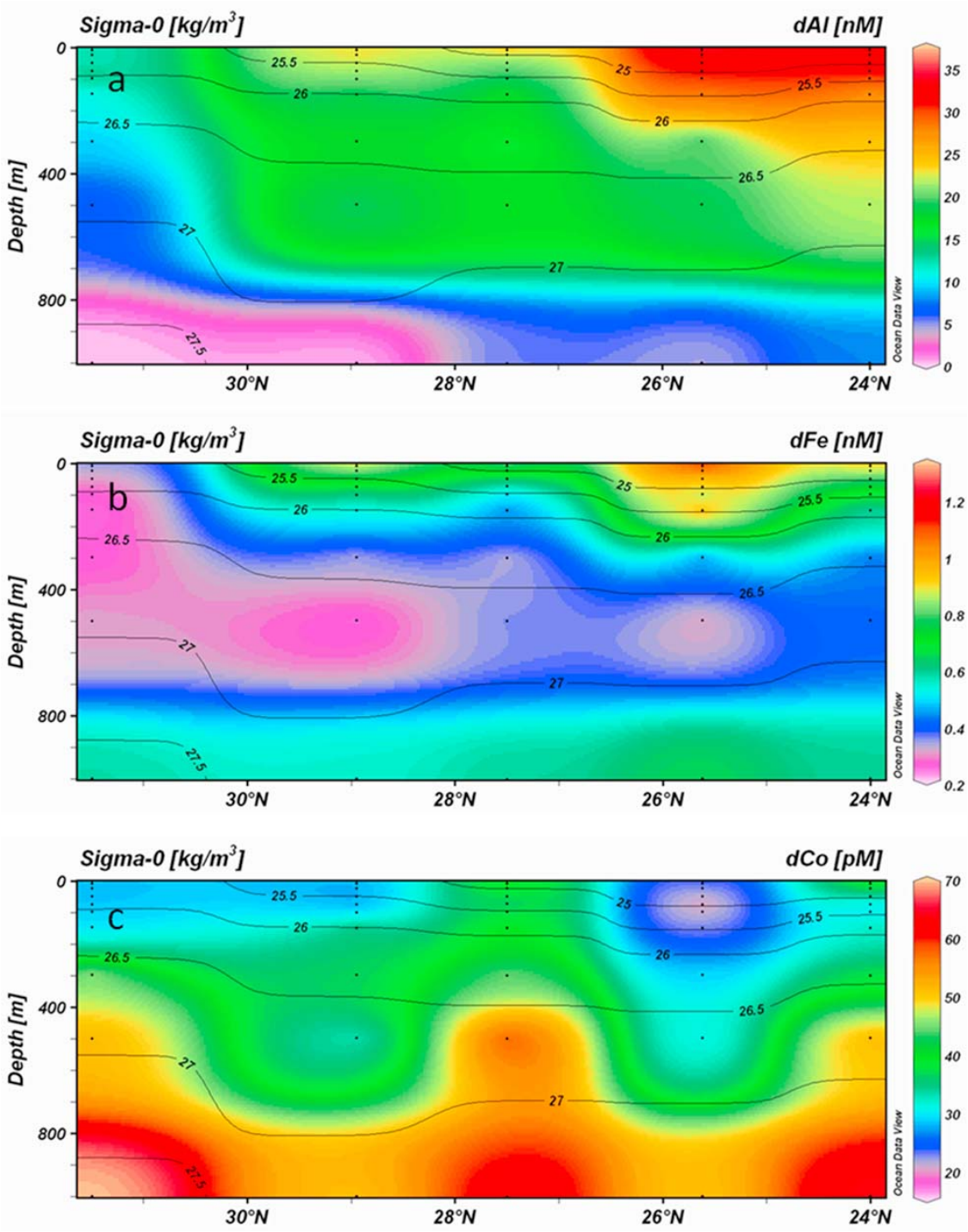

Figure 6. Interpolated vertical sections of (a) dAl, (b) dFe and (c) dCo along the cruise track, showing water column data only. Interpolated potential density (sigma-θ) contours are overlaid on each.

Pacific, although sea surface concentrations are 8–40 times lower in the Pacific, which is thought to reflect the lower dust inputs to that oceanic region [*Orians and Bruland*, 1986].

[34] Similar vertical distributions were observed for dFe, which also has a strong aeolian source, and is thought to be scavenged from the water column, with an apparently shorter residence time than dAl [*Johnson et al.*, 1997; *Jickells*, 1999; *Bergquist and Boyle*, 2006; *Boyd and Ellwood*, 2010]. The water column dFe profiles (Figures 5b and 6b) all show a surface enrichment that generally increased from north to south (~0.4–1.3 nM), as observed for the surface transect samples, as well as sub-surface minima (~0.2–0.4 nM) at depths that range from ~150 m (K1) to ~500 m (K2 and K4). However, the distribution of dFe differs from that of dAl in two respects. The first is the 'nutrient-type' behavior

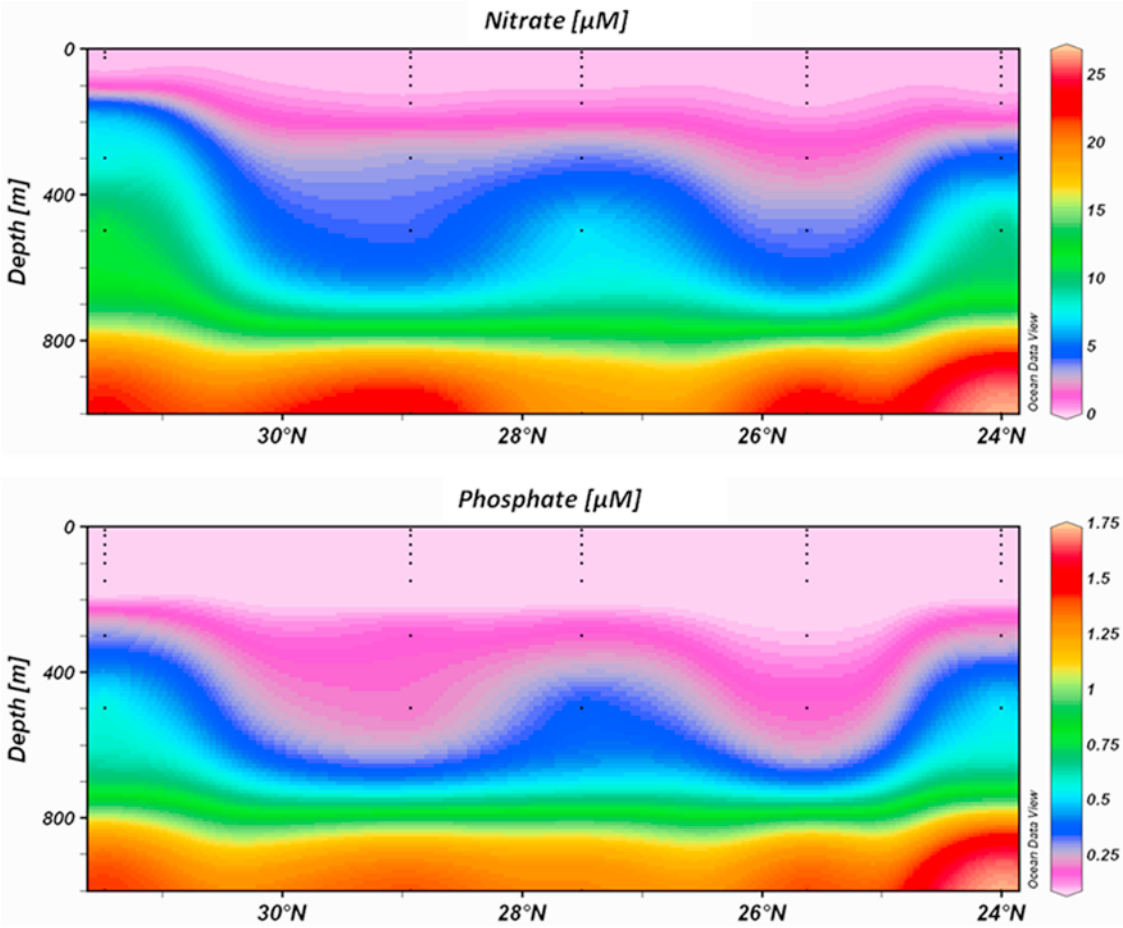

Figure 7. Interpolated vertical sections of nitrate and phosphate along the cruise track, based on analysis of water column samples collected at trace metal sampling stations.

of dFe [*Johnson et al.*, 1997; *Jickells*, 1999; *Boyd and Ellwood*, 2010], which is reflected in the secondary concentration maxima in our deepest samples (1000 m), and the sub-surface dFe minimum coincident with the deep fluorescence maximum at station K1, as previously described for the subtropical North Atlantic [*Sedwick et al.*, 2005; *Measures et al.*, 2008]. Second, the meridional dFe section (Figure 6b) reveals the greatest surface dFe enrichments at stations K2 and K4, which were both located in anticyclonic eddies. We hypothesize that these surface maxima are the indirect result of nutrient deficiency within these eddies, due to depression of the pycnocline and nutricline (Figures 6 and 7), which inhibits biological production and the associated removal of aeolian dFe from the water column [*Sedwick et al.*, 2005]. Conversely, the upwelling of nutrients within the cyclonic eddy at station K1 may have enhanced biological production [*McGillicuddy et al.*, 2007], thus contributing to the depletion of dFe within the euphotic zone.

[35] Previous studies in the subtropical North Atlantic and Pacific suggest that dCo follows a hybrid of nutrient- and scavenged-type behavior in the upper water column. [*Moffett and Ho*, 1996; *Saito and Moffett*, 2002; *Noble et al.*, 2008]. Our water column and surface water dCo data are generally consistent with these observations, with the vertical profiles (Figure 5c) and interpolated vertical section (Figure 6c) of dCo revealing a nutrient-like distribution similar to those of dissolved nitrate and phosphate (Figure 7). The water column profiles (Figure 5c) show dCo minima of ~20–30 pM located at a similar depth to the sub-surface chlorophyll maximum (see section 3.5, below), below which dCo concentrations increase to maximum concentrations of ~50–70 nM at our deepest sampling depth of 1000 m. The water column dCo profiles show surface concentrations that were slightly elevated relative to the sub-surface euphotic zone (Figure 5c). Moreover, the dCo sectional plot (Figure 6c) reveals an increase of ~10 pM in surface dCo concentrations from north to south, with the exception of the anticylonic eddy that was sampled at station K4.

[36] This subtle meridional gradient in surface dCo concentration, which is not readily discerned in our near-surface underway samples (Figure 3), is roughly consistent with our estimates of aeolian dCo input that are discussed in section 3.4. This then suggests that dust deposition may constitute a significant source of dCo to surface waters in the Sargasso Sea, particularly during the late summer, when aerosol Co loadings are likely to be higher than the period during and prior to the *FeAST*-6 cruise in early June. The water column profiles from station K5 provide support for

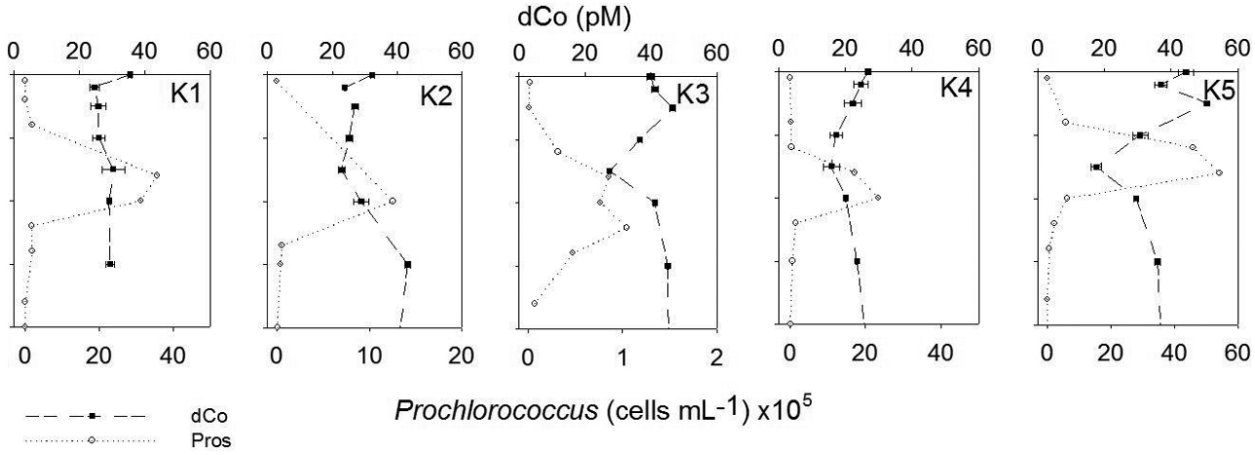

Figure 8. *Prochlorococcus* (Pros) abundance (cells mL^{-1}) $\times 10^5$ versus dCo concentration (pM; $\pm$ 1σ) for the euphotic zone of stations K1–K5. Minimum dCo was observed at depths in the region of maximum abundances of *Prochlorococcus* at all stations except station K1 (see text). Note the different scales for *Prochlorococcus* abundance.

this idea, in that the dCo concentrations within the surface mixed layer (~40 pM) are similar to those near the base of the seasonal thermocline (Figures 2 and 5). A particularly striking feature of the water column dCo data is the pronounced concentration minimum centered at ~100 m depth at station K4. Given its association with strong surface nutrient depletion mediated by an anticyclonic eddy, this feature would appear to provide evidence of the primarily nutrient-like behavior of dCo, suggesting that limited vertical resupply within this eddy has resulted in extreme biological drawdown of this essential micronutrient [e.g., see *Moffett and Ho*, 1996], likely a result of increased scavenging due to recently deposited dust particles and/or enhanced biological productivity due to the higher dFe concentrations within the lower euphotic zone at station K4 relative to the other stations.

[37] Finally, we note that the chemical speciation of dCo may play a role in maintaining low dCo concentrations in the surface mixed layer, relative to dFe. The concentrations of dCo and dFe are both subject to thermodynamic solubility limits, which are effectively increased when a proportion of the dissolved metal pool is complexed by organic ligands [*Liu and Millero*, 1999; *Saito and Moffett*, 2001]. In surface waters of the Sargasso Sea, iron-binding ligands appear to exceed dFe concentrations [*Cullen et al.*, 2006; J. T. Cullen, unpublished data, 2008], thus maintaining dFe concentrations in excess of the thermodynamic solubility of Fe(III). *Saito and Moffett* [2001] observed similar dCo and cobalt-binding ligand abundance in this region. Therefore, there may be a limited capacity for the addition of dCo from sources such as dust and rain, despite the relatively large fraction of 'soluble' cobalt in aerosols (section 3.3). This may go some way toward explaining the clear signature of atmospheric deposition in the distribution of dFe in our study region, even though our aerosol leaches suggest a greater fractional solubility for aerosol Co versus aerosol Fe. Furthermore, if cobalt-binding ligands are biologically produced, then lateral variations in microbial biomass or community composition might be expected to modulate the distribution of cobalt-binding ligands, and thus dCo.

3.5. Phytoplankton Ecology

[38] Consistent with previous observations that suggest removal of dCo in the euphotic zone of the Sargasso Sea is dominated by biological uptake [*Moffett and Ho*, 1996; *Saito and Moffett*, 2002], we observed minimum dCo concentrations (16–28 pM) at depths near 75 m, coinciding with the maximum abundance of *Prochlorococcus* (mean = 3.1×10^6 cells mL^{-1}; see Figure 8). Below this depth, dCo concentrations increased, with profiles following a nutrient-like distribution (Figure 5c), as discussed in the previous section. In contrast, minimum dFe concentrations were observed near the base of, or deeper than, the euphotic zone. This most likely reflects biological Fe uptake within the sub-surface chlorophyll maximum, [*Sedwick et al.*, 2005; *Measures et al.*, 2008], which coincided with the greatest abundance of picoeukaryotes (average 570 cells mL^{-1}), as well as removal via particle scavenging below the euphotic zone.

[39] Our data hint at a possible decoupling in the biological removal of dCo and dFe from the euphotic zone. Specifically, for depths < 150 m, we observed an inverse relationship between picoeukaryotic phytoplankton abundance and dFe concentration, and between *Prochlorococcus* abundance and dCo concentration (with the exception of station K1, near BATS). Interestingly, these observations imply that *Prochlorococcus* may play an important role in removing dCo from the euphotic zone, and, conversely, that low concentrations of dCo might regulate the growth rate and biomass of *Prochlorococcus* in the Sargasso Sea. *Prochlorococcus* has an absolute cellular requirement for cobalt; given a standing stock of 10^5 cells mL^{-1} of *Prochlorococcus* growing at 0.4 d^{-1} in the Sargasso Sea [*Mann and Chisholm*, 2000], *Saito et al.* [2002] have estimated that 0.3 pM L^{-1} d^{-1} of dCo would be incorporated into new cells, which, over a seasonal timescale, may represent a large fraction of the dCo inventory of the euphotic zone. This then suggests that *Prochlorococcus* could be a major sink for dCo in surface waters of the Sargasso Sea.

[40] In this regard, we note that data from the subtropical North Pacific have been used to argue that cobalt associated

with sinking biogenic particles may be rapidly remineralized, and thus recycled by autotrophs in the euphotic zone [*Noble et al.*, 2008]. Certainly, such recycling of cobalt is consistent with the vertical distribution of dCo compared with dFe (Figure 6), which suggest the greater importance of particle scavenging as a sink for dFe below the euphotic zone. Such recycling would provide a mechanism to resupply dCo to the euphotic zone during summer in the absence of a strong atmospheric source of Co (in contrast to Fe).

4. Conclusions

[41] Overall, our data set demonstrates that dCo exhibits primarily nutrient-like behavior in surface waters of the Sargasso Sea, in accord with results of previous studies. Analyses of aerosol samples indicate a high fractional solubility of aerosol Co (8–100%), relative to Fe (0.44–45%), although the total aerosol loadings suggest that the atmospheric input of dCo to surface waters is modest, even allowing for a potentially large fraction in wet deposition. This conclusion is consistent with our water column data, which appear to show the impact of atmospheric deposition to our most southerly sampling locations, where dust loadings are likely to be higher. This further implies that atmospheric deposition might account for a significant input of dCo to the surface ocean during late summer, when the Sargasso Sea receives its greatest inputs of Saharan dust. However, further seasonal-scale sampling is required to assess the relative importance of atmospheric deposition versus vertical resupply for dCo in the Sargasso Sea. Finally, ancillary biological observations suggest that *Prochlorococcus* could play a major role in removing dCo from the euphotic zone, and that dCo availability might regulate primary production by *Prochlorococcus* in the Sargasso Sea.

[42] **Acknowledgments.** The authors thank Mak Saito for his insightful and constructive review, the captain and crew of the RV *Atlantic Explorer* for their excellent shipboard support, and Dennis McGillicuddy and Valery Kosnyrev for providing near real-time satellite altimetry analyses. The NOAA Air Resources Laboratory (ARL) HYSPLIT atmospheric transport and dispersion model (http://www.arl.noaa.gov/ready.php) was used for simulation of the air mass back trajectories presented in this manuscript. The ICP-MS measurements of atmospheric samples were carried out in WHOI's Plasma Facility under the supervision of S. Birdwhistell. This study was supported by a University of Plymouth, Marine Institute scholarship to R.U.S., a U.S. National Science Foundation grant to P.N.S. (OCE-0550594), T.M.C. (OCE-0550592) and E.R.S. (OCE-0549954), and a European Commission Marie Curie Outgoing International Fellowship under contract PIOF-GA-2009-235418 SOLAIROS for S.J.U.

References

Arimoto, R., R. Duce, B. Ray, and C. Unni (1985), Atmospheric trace elements at Enewetak Atoll: 2. Transport to the ocean by wet and dry deposition, *J. Geophys. Res.*, *90*, 2391–2408, doi:10.1029/JD090iD01p02391.

Arimoto, R., R. A. Duce, B. J. Ray, W. G. Ellis Jr., J. T. Cullen, and J. T. Merrill (1995), Trace elements in the atmosphere over the North Atlantic, *J. Geophys. Res.*, *100*, 1199–1213, doi:10.1029/94JD02618.

Arimoto, R., R. A. Duce, B. J. Ray, and U. Tomza (2003), Dry deposition of trace elements to the western North Atlantic, *Global Biogeochem. Cycles*, *17*(1), 1010, doi:10.1029/2001GB001406.

Baker, A. R., and T. D. Jickells (2006), Mineral particle size as a control on aerosol iron solubility, *Geophys. Res. Lett.*, *33*, L17608, doi:10.1029/2006GL026557.

Baker, A. R., T. D. Jickells, M. Witt, and K. L. Linge (2006), Trends in the solubility of iron, aluminium, manganese and phosphorus in aerosol collected over the Atlantic Ocean, *Mar. Chem.*, *98*, 43–58, doi:10.1016/j.marchem.2005.06.004.

Baker, A. R., K. Weston, S. D. Kelly, M. Voss, P. Streu, and J. N. Cape (2007), Dry and wet deposition of nutrients from the tropical Atlantic atmosphere: Links to primary productivity and nitrogen fixation, *Deep Sea Res., Part I*, *54*, 1704–1720, doi:10.1016/j.dsr.2007.07.001.

Bergquist, B. A., and E. A. Boyle (2006), Dissolved iron in the tropical and subtropical Atlantic Ocean, *Global Biogeochem. Cycles*, *20*, GB1015, doi:10.1029/2005GB002505.

Bertrand, E. M., et al. (2007), Vitamin B_{12} and iron co-limitation of phytoplankton growth in the Ross Sea, *Limnol. Oceanogr.*, *52*, 1079–1093, doi:10.4319/lo.2007.52.3.1079.

Boyd, P. W., and M. J. Ellwood (2010), The biogeochemical cycle of iron in the ocean, *Nat. Geosci.*, *3*, 675–682, doi:10.1038/ngeo964.

Boyd, P. W., et al. (2000), A mesoscale phytoplankton bloom in the polar Southern Ocean stimulated by iron fertilization, *Nature*, *407*, 695–702, doi:10.1038/35037500.

Brown, M. T., and K. W. Bruland (2008), An improved flow-injection analysis method for the determination of dissolved aluminum in seawater, *Limnol. Oceanogr. Methods*, *6*, 87–95, doi:10.4319/lom.2008.6.87.

Bruland, K. W., E. L. Rue, G. J. Smith, and G. R. DiTullio (2005), Iron, macronutrients and diatom blooms in the Peru upwelling regime: Brown and blue waters of Peru, *Mar. Chem.*, *93*, 81–103, doi:10.1016/j.marchem.2004.06.011.

Buck, C. S., W. M. Landing, J. A. Resing, and G. T. Lebon (2006), Aerosol iron and aluminum solubility in the northwest Pacific Ocean: Results from the 2002 IOC cruise, *Geochem. Geophys. Geosyst.*, *7*, Q04M07, doi:10.1029/2005GC000977.

Campbell, L., H. A. Nolla, and D. Vaulot (1994), The importance of *Prochlorococcus* to community structure in the central North Pacific Ocean, *Limnol. Oceanogr.*, *39*, 954–961, doi:10.4319/lo.1994.39.4.0954.

Cembella, A. D., N. J. Antia, and P. J. Harrison (1982), The utilization of inorganic and organic phosphorous compounds as nutrients by eukaryotic microalgae: A multidisciplinary perspective: Part I, *Crit. Rev. Microbiol.*, *10*, 317–391, doi:10.3109/10408418209113567.

Chen, L., and R. A. Duce (1983), The sources of sulfate, vanadium and mineral matter in aerosol particles over Bermunda, *Atmos. Environ.*, *17*, 2055–2064, doi:10.1016/0004-6981(83)90362-1.

Coale, K. H., et al. (1996), A massive phytoplankton bloom induced by an ecosystem-scale iron fertilization experiment in the equatorial Pacific Ocean, *Nature*, *383*, 495–501, doi:10.1038/383495a0.

Croft, M. T., A. D. Lawrence, E. Raux-Deery, M. J. Warren, and A. G. Smith (2005), Algae acquire vitamin B_{12} through a symbiotic relationship with bacteria, *Nature*, *438*, 90–93, doi:10.1038/nature04056.

Cullen, J. T., B. A. Bergquist, and J. W. Moffett (2006), Thermodynamic characterization of the partitioning of iron between soluble and colloidal species in the Atlantic Ocean, *Mar. Chem.*, *98*, 295–303, doi:10.1016/j.marchem.2005.10.007.

Duce, R. A., and G. L. Hoffman (1976), Atmospheric vanadium transport to the ocean, *Atmos. Environ.*, *10*, 989–996, doi:10.1016/0004-6981(76)90207-9.

Duce, R. A., and N. W. Tindale (1991), Atmospheric transport of iron and its deposition to the ocean, *Limnol. Oceanogr.*, *36*, 1715–1726, doi:10.4319/lo.1991.36.8.1715.

Ellwood, M. J., and C. M. G. van den Berg (2001), Determination of organic complexation of cobalt in seawater by cathodic stripping voltammetry, *Mar. Chem.*, *75*, 33–47, doi:10.1016/S0304-4203(01)00024-X.

Gao, Y., Y. J. Kaufman, D. Tanre, D. Kolber, and P. Falkowski (2001), Seasonal distributions of aeolian iron fluxes to the global ocean, *Geophys. Res. Lett.*, *28*, 29–32, doi:10.1029/2000GL011926.

Gledhill, M., and C. M. G. van den Berg (1994), Determination of complexation of iron(III) with natural organic complexing ligands in seawater using cathodic stripping voltammetry, *Mar. Chem.*, *47*, 41–54.

Goericke, R., and N. A. Welschmeyer (1993), The marine prochlorophyte *Prochlorococcus* contributes significantly to phytoplankton biomass and primary production in the Sargasso Sea, *Deep Sea Res., Part I*, *40*, 2283–2294, doi:10.1016/0967-0637(93)90104-B.

Gong, N., et al. (2005), Characterization of a thermostable alkaline phosphatase from a novel species *Thermus yunnanensis* sp. nov. and investigation of its cobalt activation at high temperature, *Biochim. Biophys. Acta*, *1750*, 103–111.

Helmers, E., and O. Schrems (1995), Wet deposition of metals to the tropical North and the South Atlantic Ocean, *Atmos. Environ.*, *29*, 2475–2484, doi:10.1016/1352-2310(95)00159-V.

Huang, S., K. A. Rahn, R. Arimoto, W. C. Graustein, and K. K. Turekian (1999), Semiannual cycles of pollution at Bermuda, *J. Geophys. Res.*, *104*, 30,309–30,317, doi:10.1029/1999JD900801.

Jakuba, R. W., J. W. Moffett, and S. T. Dyhrman (2008), Evidence for the linked biogeochemical cycling of zinc, cobalt, and phosphorus in the western North Atlantic Ocean, *Global Biogeochem. Cycles*, *22*, GB4012, doi:10.1029/2007GB003119.

Jickells, T. (1999), The inputs of dust derived elements to the Sargasso Sea; a synthesis, *Mar. Chem.*, *68*, 5–14, doi:10.1016/S0304-4203(99)00061-4.

Jickells, T. D., and J. D. Burton (1988), Cobalt, copper, manganese and nickel in the Sargasso Sea, *Mar. Chem.*, *23*, 131–144, doi:10.1016/0304-4203(88)90027-8.

Jickells, T., T. Church, A. Véron, and R. Arimoto (1994), Atmospheric inputs of manganese and aluminium to the Sargasso Sea and their relation to surface water concentrations, *Mar. Chem.*, *46*, 283–292, doi:10.1016/0304-4203(94)90083-3.

Jickells, T. D., et al. (2005), Global iron connections between desert dust, ocean biogeochemistry and climate, *Science*, *308*, 67–71, doi:10.1126/science.1105959.

Johnson, K. S., R. M. Gordon, and K. H. Coale (1997), What controls dissolved iron concentrations in the world ocean?, *Mar. Chem.*, *57*, 137–161, doi:10.1016/S0304-4203(97)00043-1.

Knauer, G. A., J. H. Martin, and R. M. Gordon (1982), Cobalt in north-east Pacific waters, *Nature*, *297*, 49–51, doi:10.1038/297049a0.

Lane, T. W., and F. M. M. Morel (2000), Regulation of carbonic anhydrase expression by zinc, cobalt, and carbon dioxide in the marine diatom *Thalassiosira weissflogii*, *Plant Physiol.*, *123*, 345–352, doi:10.1104/pp.123.1.345.

Liu, X., and F. J. Millero (1999), The solubility of iron hydroxide in sodium chloride solutions, *Geochim. Cosmochim. Acta*, *63*, 3487–3497, doi:10.1016/S0016-7037(99)00270-7.

Mackie, D. S., P. W. Boyd, K. Hunter, and G. H. McTainsh (2005), Simulating the cloud processing of iron in Australian dust: pH and dust concentration, *Geophys. Res. Lett.*, *32*, L06809, doi:10.1029/2004GL022122.

Mackie, D. S., J. M. Peat, G. H. McTainsh, P. W. Boyd, and K. A. Hunter (2006), Soil abrasion and eolian dust production: Implications for iron partitioning and solubility, *Geochem. Geophys. Geosyst.*, *7*, Q12Q03, doi:10.1029/2006GC001404.

Mann, E. L., and S. W. Chisholm (2000), Iron limits the cell division rate of *Prochlorococcus* in the eastern equatorial Pacific, *Limnol. Oceanogr.*, *45*, 1067–1076, doi:10.4319/lo.2000.45.5.1067.

Martin, J. H., G. H. Knauer, D. M. Karl, and W. W. Broenkow (1987), VERTEX: Carbon cycling in the northeast Pacific, *Deep Sea Res., Part A*, *34*, 267–285, doi:10.1016/0198-0149(87)90086-0.

Mather, R. L., et al. (2008), Phosphorus cycling in the North and South Atlantic Ocean subtropical gyres, *Nat. Geosci.*, *1*, 439–443, doi:10.1038/ngeo232.

McGillicuddy, D. J., et al. (2007), Eddy/wind interactions stimulate extraordinary mid-ocean plankton blooms, *Science*, *316*, 1021–1026, doi:10.1126/science.1136256.

Measures, C. I., and M. T. Brown (1996), Estimating dust input to the Atlantic Ocean using surface water Al concentrations, in *The Impact of Desert Dust Across the Mediterranean*, edited by S. Guerzoni and R. Chester, pp. 301–311, Kluwer, Dordrecht, Netherlands.

Measures, C. I., and S. Vink (2000), On the use of dissolved aluminum in surface waters to estimate dust deposition to the ocean, *Global Biogeochem. Cycles*, *14*, 317–327, doi:10.1029/1999GB001188.

Measures, C. I., J. M. Edmond, and T. D. Jickells (1986), Aluminium in the northwest Atlantic, *Geochim. Cosmochim. Acta*, *50*, 1423–1429, doi:10.1016/0016-7037(86)90315-7.

Measures, C. I., J. Yuan, and J. A. Resing (1995), Determination of iron in seawater by flow injection analysis using in-line preconcentration and spectrophotometric detection, *Mar. Chem.*, *50*, 3–12, doi:10.1016/0304-4203(95)00022-J.

Measures, C. I., W. M. Landing, W. T. Brown, and C. S. Buck (2008), High-resolution Al and Fe data from the Atlantic Ocean CLIVAR-CO_2 Repeat Hydrography A16N transect: Extensive linkages between atmospheric dust and upper ocean geochemistry, *Global Biogeochem. Cycles*, *22*, GB1005, doi:10.1029/2007GB003042.

Moffett, J. W., and J. Ho (1996), Oxidation of cobalt and manganese in seawater via a common microbially catalyzed pathway, *Geochim. Cosmochim. Acta*, *60*, 3415–3424, doi:10.1016/0016-7037(96)00176-7.

Moody, J. L., S. J. Oltmans, H. Levy II, and J. T. Merrill (1995), Transport climatology of tropospheric ozone: Bermuda, 1988–1991, *J. Geophys. Res.*, *100*, 7179–7194, doi:10.1029/94JD02830.

Moore, J. K., and O. Braucher (2008), Sedimentary and mineral dust sources of dissolved iron to the world ocean, *Biogeosciences*, *5*, 631–656, doi:10.5194/bg-5-631-2008.

Morel, F. M. M., et al. (1994), Zinc and carbon co-limitation of marine phytoplankton, *Nature*, *369*, 740–742, doi:10.1038/369740a0.

Noble, A. E., M. A. Saito, K. Maiti, and C. Benitez-Nelson (2008), Cobalt, manganese, and iron near the Hawaiian Islands: A potential concentrating mechanism for cobalt within a cyclonic eddy and implications for the hybrid-type trace metals, *Deep Sea Res., Part II*, *55*, 1473–1490, doi:10.1016/j.dsr2.2008.02.010.

Olson, R. J., E. R. Zettler, and M. D. DuRand (1993), Phytoplankton analysis using flow cytometry, in *Handbook of Methods in Aquatic Microbial Ecology*, edited by P. F. Kemp et al., pp. 175–186, Lewis, Boca Raton, Fla.

Orians, K. J., and K. W. Bruland (1986), The biogeochemistry of aluminum in the Pacific Ocean, *Earth Planet. Sci. Lett.*, *78*, 397–410, doi:10.1016/0012-821X(86)90006-3.

Panzeca, C., et al. (2008), Potential cobalt limitation of vitamin B_{12} synthesis in the North Atlantic Ocean, *Global Biogeochem. Cycles*, *22*, GB2029, doi:10.1029/2007GB003124.

Partensky, F., W. R. Hess, and D. Vaulot (1999), *Prochlorococcus*, a marine photosynthetic prokaryote of global significance, *Microbiol. Mol. Biol. Rev.*, *63*, 106–127.

Plocke, D. J., C. Levinthal, and B. L. Vallee (1962), Alkaline phosphatase of *Escherichia coli*: A zinc metalloenzyme, *Biochemistry*, *1*, 373–378, doi:10.1021/bi00909a001.

Prospero, J. M., and T. N. Carlson (1972), Vertical and areal distribution of Saharan dust over the equatorial North Atlantic Ocean, *J. Geophys. Res.*, *77*, 5255–5265, doi:10.1029/JC077i027p05255.

Prospero, J. M., R. A. Glaccum, and R. T. Nees (1981), Atmospheric transport of soil dust from Africa to South America, *Nature*, *289*, 570–572, doi:10.1038/289570a0.

Resing, J. A., and C. I. Measures (1994), Fluorometric determination of Al in seawater by flow injection analysis with in-line preconcentration, *Anal. Chem.*, *66*, 4105–4111, doi:10.1021/ac00094a039.

Rue, E. L., and K. W. Bruland (1997), The role of organic complexation on ambient iron chemistry in the equatorial Pacific Ocean and the response of a mesoscale iron addition experiment, *Limnol. Oceanogr.*, *42*, 901–910, doi:10.4319/lo.1997.42.5.0901.

Saito, M. A., and T. J. Goepfert (2008), Zinc-cobalt colimitation of *Phaeocystis antarctica*, *Limnol. Oceanogr.*, *53*, 266–275, doi:10.4319/lo.2008.53.1.0266.

Saito, M. A., and J. W. Moffett (2001), Complexation of cobalt by natural organic ligands in the Sargasso Sea as determined by a new high-sensitivity electrochemical cobalt speciation method suitable for open ocean work, *Mar. Chem.*, *75*, 49–68, doi:10.1016/S0304-4203(01)00025-1.

Saito, M. A., and J. W. Moffett (2002), Temporal and spatial variability of cobalt in the Atlantic Ocean, *Geochim. Cosmochim. Acta*, *66*, 1943–1953, doi:10.1016/S0016-7037(02)00829-3.

Saito, M. A., J. W. Moffett, S. Chisholm, and J. B. Waterbury (2002), Cobalt limitation and uptake in *Prochlorococcus*, *Limnol. Oceanogr.*, *47*, 1629–1636, doi:10.4319/lo.2002.47.6.1629.

Saito, M. A., J. W. Moffet, and G. R. DiTullio (2004), Cobalt and nickel in the Peru upwelling region: A major flux of labile cobalt utilized as a micronutrient, *Global Biogeochem. Cycles*, *18*, GB4030, doi:10.1029/2003GB002216.

Saito, M. A., G. Rocap, and J. W. Moffett (2005), Production of cobalt binding ligands in a *Synechococcus* feature at the Costa Rica upwelling dome, *Limnol. Oceanogr.*, *50*, 279–290, doi:10.4319/lo.2005.50.1.0279.

Saito, M. A., T. J. Goepfert, and J. T. Ritt (2008), Some thoughts on the concept of colimitation: Three definitions and the importance of bioavailability, *Limnol. Oceanogr.*, *53*, 276–290, doi:10.4319/lo.2008.53.1.0276.

Sedwick, P. N., et al. (2005), Iron in the Sargasso Sea (Bermuda Atlantic Time-series Study region) during summer: Eolian imprint, spatiotemporal variability, and ecological implications, *Global Biogeochem. Cycles*, *19*, GB4006, doi:10.1029/2004GB002445.

Sedwick, P. N., E. R. Sholkovitz, and T. M. Church (2007), Impact of anthropogenic combustion emissions on the fractional solubility of aerosol iron: Evidence from the Sargasso Sea, *Geochem. Geophys. Geosyst.*, *8*, Q10Q06, doi:10.1029/2007GC001586.

Sedwick, P. N., A. R. Bowie, and T. W. Trull (2008), Dissolved iron in the Australian sector of the Southern Ocean (CLIVAR-SR3 section): Meridional and seasonal trends, *Deep Sea Res., Part I*, *55*, 911–925, doi:10.1016/j.dsr.2008.03.011.

Shelley, R. U., B. Zachhuber, P. J. Sedwick, P. J. Worsfold, and M. C. Lohan (2010), Determination of total dissolved cobalt in UV-irradiated seawater using flow injection with chemiluminescence detection, *Limnol. Oceanogr. Methods*, *8*, 352–362, doi:10.4319/lom.2010.8.352.

Sholkovitz, E. R., and P. N. Sedwick (2006), Open-ocean deployment of a buoy-mounted aerosol sampler on the Bermuda Testbed Mooring: Aerosol iron and sea salt over the Sargasso Sea, *Deep Sea Res., Part I*, *53*, 547–560, doi:10.1016/j.dsr.2005.12.002.

Sholkovitz, E. R., P. N. Sedwick, and T. M. Church (2009), Influence of anthropogenic combustion emissions on the deposition of soluble aerosol iron to the ocean: Empirical estimates for island sites in the North Atlantic, *Geochim. Cosmochim. Acta*, *73*, 3981–4003, doi:10.1016/j.gca.2009.04.029.

Sholkovitz, E. R., P. N. Sedwick, and T. M. Church (2010), On the fractional solubility of copper in marine aerosols: Toxicity of aeolian copper revisited, *Geophys. Res. Lett.*, *37*, L20601, doi:10.1029/2010GL044817.

Siegel, D. A., D. J. McGillicuddy, and E. A. Fields (1999), Mesoscale eddies, satellite altimetry, and new production in the Sargasso Sea, *J. Geophys. Res.*, *104*, 13,359–13,379, doi:10.1029/1999JC900051.

Smirnov, A., et al. (2002), Optical properties of atmospheric aerosol in maritime environments, *J. Atmos. Sci.*, *59*, 501–523, doi:10.1175/1520-0469(2002)059<0501:OPOAAI>2.0.CO;2.

Steinberg, D. K., et al. (2001), Overview of the US JGOFS Bermuda Atlantic Time-series Study (BATS): A decade-scale look at ocean biology and biogeochemistry, *Deep Sea Res., Part II*, *48*, 1405–1447, doi:10.1016/S0967-0645(00)00148-X.

Stumm, W., and J. J. Morgan (1996), *Aquatic Chemistry: Chemical Equilibria and Rates in Natural Waters*, John Wiley, Chichester, U. K.

Sunda, W. G., and S. A. Huntsman (1995), Cobalt and zinc interreplacement in marine phytoplankton: Biological and geochemical implications, *Limnol. Oceanogr.*, *40*, 1404–1417, doi:10.4319/lo.1995.40.8.1404.

Thuróczy, C.-E., M. Boyé, and R. Losno (2010), Dissolution of cobalt and zinc from natural and anthropogenic dusts in seawater, *Biogeosciences*, *7*, 1927–1936, doi:10.5194bg-7-1927-2010.

Tian, Z., P. Olliver, A. Véron, and T. M. Church (2008), Atmospheric Fe deposition modes at Bermuda and the adjacent Sargasso Sea, *Geochem. Geophys. Geosyst.*, *9*, Q08007, doi:10.1029/2007GC001868.

van den Berg, C. M. G. (1995), Evidence for organic complexation of iron in seawater, *Mar. Chem.*, *50*, 139–157, doi:10.1016/0304-4203(95)00032-M.

Véron, A. J., and T. M. Church (1997), Use of stable lead isotopes and trace metals to characterize air mass sources into the eastern North Atlantic, *J. Geophys. Res.*, *102*, 28049–28058, doi:10.1029/97JD01527.

Vink, S., and C. I. Measures (2001), The role of dust deposition in determining surface water distributions of Al and Fe in the South West Atlantic, *Deep Sea Res., Part II*, *48*, 2787–2809, doi:10.1016/S0967-0645(01)00018-2.

Wu, J., and E. Boyle (2002), Iron in the Sargasso Sea: Implications for the processes controlling dissolved Fe distribution in the ocean, *Global Biogeochem. Cycles*, *16*(4), 1086, doi:10.1029/2001GB001453.

Zubkov, M. V., and P. H. Burkill (2006), Syringe pumped high speed flow cytometry of oceanic phytoplankton, *Cytometry A*, *69A*, 1010–1019, doi:10.1002/cyto.a.20332.